

From Time Series to Euclidean Spaces: On Spatial Transformations for Temporal Clustering

Nuno Mota Goncalves
IBM Research - Zurich
glv@zurich.ibm.com

Ioana Giurgiu
IBM Research - Zurich
igi@zurich.ibm.com

Anika Schumann
IBM Research - Zurich
ikh@zurich.ibm.com

Abstract

Unsupervised clustering of temporal data is both challenging and crucial in machine learning. In this paper, we show that neither traditional clustering methods, time series specific or even deep learning-based alternatives generalize well when both varying sampling rates and high dimensionality are present in the input data. We propose a novel approach to temporal clustering, in which we (1) transform the input time series into a distance-based projected representation by using similarity measures suitable for dealing with temporal data, (2) feed these projections into a multi-layer CNN-GRU autoencoder to generate meaningful domain-aware latent representations, which ultimately (3) allow for a natural separation of clusters beneficial for most important traditional clustering algorithms. We evaluate our approach on time series datasets from various domains and show that it not only outperforms existing methods in all cases, by up to 32%, but is also robust and incurs negligible computation overheads.

Introduction

One major concern in machine learning is how to handle data with temporal characteristics - or *time series*. Such data exists in staggering amounts in almost every field, from sensors, social networks, IoT, human mobility, finance or even medicine (Aghabozorgi, Shirkhorshidi, and Wah 2015; Aljalbout et al. 2018). Unlike static data, there exist strong temporal and spatial dependencies (e.g., correlated time series), so an appropriate treatment of these properties becomes critical in any temporal data processing. Among all techniques applied to time series, *unsupervised clustering* is the most widely used for two main reasons. First, it does not require costly supervision or time-consuming annotation of data (Paparrizos and Gravano 2015). Second, it not only is a powerful stand-alone exploratory method but also proved to be a useful pre-processing or post-processing step for other tasks (e.g., anomaly detection).

In the literature, various approaches for clustering temporal data have been proposed. When the time series have the same length and are sampled at the same frequency, methods like k-means, which employ the Euclidean distance, can

be used (Besse et al. 2015; Aggarwal and Reddy 2014). However, most times the problem of time series clustering remains challenging as typically temporal data originating from different domains shows significant variations in dimensionality and temporal scales. To tackle different sampling rates, elastic distance metrics such as dynamic time warping (DTW) (Sakoe and Chiba 1978) or cross-correlation metrics such as SBD, used in k-shape (Paparrizos and Gravano 2015), are frequently used. However, these metrics suffer from high-dimensionality in univariate spaces (e.g., long temporal sequences, where either the computation costs become intractable or an optimal alignment becomes non-trivial and possibly ambiguous). This effect is especially exacerbated for multivariate time series.

In other domains, dimensionality reduction performed by autoencoders (AEs) has allowed for several improvements in unsupervised classification (Xie, Girshick, and Farhadi 2016; Guo et al. 2017; Shah and Koltun 2017; Yang et al. 2017; Zhang et al. 2017; Yang, Parikh, and Batra 2016; Dizaji et al. 2017; Chazan, Gannot, and Goldberger 2018). The idea is to generate lower-dimensional latent representations that are then fed into a customized layer responsible for the clustering task (i.e., typically by minimizing clustering loss via Kullback-Leibler (KL) divergence). When applied to image and text benchmarks, these approaches significantly outperform traditional methods. However, despite their achievements, they still lack a principled cross-domain generalization. First, they depend on standard target distributions (required by KL divergence) which requires tuning for each data type. Second, they have an implicit expectation as to the latent spaces' descriptiveness of the target domain (i.e., samples that should be clustered together would be closely represented in the latent space). This may not hold if models capture undesirable properties of the data (e.g., artifacts) or in spaces where spacial proximity is a sub-optimal measure of sample similarity (e.g., the time domain).

In this paper we postulate that all existing approaches suffer from significant drawbacks when applied in time series clustering, since: (1) traditional clustering methods cannot deal well with varying sampling rates and lengths; (2) domain-specific clustering approaches greatly suffer from high dimensionality in the sample space; and (3) AE-based

methods have no guarantees to generate meaningful latent representations. Instead, we propose a deep temporal clustering approach that focuses exclusively on generating latent spaces that naturally separate clusters, while at the same time preserving domain-specific characteristics of the data. We achieve this by:

- feeding the input space into a multi-layer CNN-GRU AE, in order to extract temporal waveforms from the original time series in a compressed format;
- before computing the reconstruction error, applying spatial transformations to both the reference samples and their reconstructed counterparts to guide the latent space construction;
- using the embeddings into a final clustering step, where any traditional clustering method could be used (e.g., k-means, spectral, DBSCAN).

In this paper, we demonstrate that by combining spatial transformations with a multi-layer CNN-GRU AE, we can generalize Euclidean metric-based clustering algorithms to potentially non-euclidean domains. We evaluate our approach on time series datasets from various sources and show that it outperforms existing methods in all cases, both in terms of accuracy (up to an 32% boost) and robustness in parameterization - while incurring small or negligible computation overheads.

Related Work

Distance metrics-based clustering – Measuring the distance between different time series needs to take into consideration the temporal correlation between the data points in a time series and the complex nature of the noise that may be present. Such noise can, for instance, be represented by different sampling rates (Yin et al. 2014). In the simplest case, when the time series have the same length and are sampled at the same frequency, general clustering methods based on Euclidean distance, such as k-means, can be used (Besse et al. 2015). However, these do not perform well when sampling rates between comparing time series are different. In this case, elastic distance measures such as dynamic time warping (DTW) (Sakoe and Chiba 1978), edit distance on real sequence (EDR) (Chen, Ozsu, and Oria 2005) or edit distance with real penalty (ERP) (Chen and Ng 2004), as well as cross-correlation measures such as the SBD metric used in k-shape (Paparrizos and Gravano 2015) are popular choices. These measures mostly focus on comparing the shape of the time series, but a recent review of most popular time series distances found that none of them is more robust than the others to all the different kinds of noise commonly present in temporal data (Wang et al. 2013).

DNN-based clustering – Deep embedding clustering approaches (Besse et al. 2015) have recently been proposed to deal with high-dimensional data, in particular images and text. For instance, DEC (Xie, Girshick, and Farhadi 2016) uses stacked denoising AEs to generate latent representations. However, spatial relationships in the reconstructed samples cannot be guaranteed. To alleviate this drawback, IDEC (Guo et al. 2017) defines a joint optimization objective that minimizes KL divergence simultaneously with

the reconstruction loss. Similar to IDEC, DCC (Shah and Koltun 2017) and DCN (Yang et al. 2017) use the reconstruction loss as part of the optimization objective. In DCC, the authors assume the number of clusters is unknown in advance and propose a clustering algorithm that continuously performs the clustering task by optimizing an objective that does not need to be updated during the optimization phase. Differently, DEPICT (Dizaji et al. 2017) uses discrete reconfigurations of datapoints to centroids and in (Yang, Parikh, and Batra 2016) the authors use agglomerative clustering. DCN uses a novel alternating stochastic gradient algorithm and a cluster structure-promoting regularization to achieve superior accuracy compared to IDEC. DAMIC (Chazan, Gannot, and Goldberger 2018) proposes an algorithm based on mixture-of-experts, where each cluster is represented by an AE. Similarly, MIXAE (Zhang et al. 2017) proposes to train simultaneously a set of AEs via a composite objective function, jointly motivating low reconstruction error and cluster identification error.

In the time series domain, deep neural networks have primarily been used for supervised learning, with few exceptions (Malhotra et al. 2017; Langkvist, Karlsson, and Loutfi 2014). However, to the best of our knowledge, there have been no efforts proposing deep learning approaches for time series clustering that are invariant to affine transformations.

Approach

Our approach is motivated by the following observations:

- traditional clustering methods, such as k-means, DBSCAN or spectral clustering are not well-suited for temporal data where varying sampling rates and sample lengths will frequently occur;
- time series specific clustering methods, such as k-means (using DTW) and k-shape, will greatly suffer from high-dimensional samples (i.e., length of time series) where an optimal alignment becomes non-trivial and possibly ambiguous;
- common deep learning approaches for dimensionality reduction, such as AEs, have no guarantees as to the meaningfulness of their latent representations, either degrading clustering accuracy for complex domains (Abid and Zou 2018) or making it unpredictable.

In this paper we take a bottom-up approach. We start by enabling domain-aware latent representations using AEs. Then, we leverage well-known temporal similarity measures and their domain-specific properties. As a last step, we propose a pipeline to better generalize traditional clustering algorithms to other (potentially non-euclidean) domains.

Meaningful Latent Spaces

Consider an unlabeled dataset S with N samples, where $S_i \in \mathbb{R}^{V \times T_i} \forall \{i \in \mathbb{N} \mid i \leq N\}$ (V being the number of variables and T_i the number of time steps specific to S_i). Generally, learning a latent representation for each input sample can easily be achieved through non-linear mappings performed by an autoencoder. These mappings can be defined as $f_W : S_i \rightarrow z_i$ and $g_W : z_i \rightarrow S'_i$, where z_i is the latent space

embedding of S_i and S'_i is the reconstruction of S_i . f_W and g_W will be learnt through a sample reconstruction error, L_r , as follows:

$$L_r(S_i, S'_i) = \frac{1}{|S_i|} \sum_j (S_{ij} - S'_{ij})^2$$

This error is nothing more than the mean squared error (MSE) between two samples. The problem with this measure is that it is analogous to Euclidean distance, arguably not the best metric for comparing time series (Aggarwal and Reddy 2014). Not only would this measure not be ideal to quantify reconstruction quality in a sample-by-sample basis, but AEs implicitly enforce that the whole reconstructed space is similar to the original space. Even if this is a desired property in other scenarios, our ultimate goal is clustering in the latent space. Therefore, our focus shifts from ensuring that the AE achieves low reconstruction error to providing relevant properties for traditional clustering, such as invariance towards geometric transformations in the input space.

To tackle the aforementioned limitations, we propose a transformation f that represents a sample as its *similarity* to each one of p randomly picked *pivot points*, detailed in lines 1–6 of Alg. 1. As such, applying f to a sample $S_i \in R^{V \times T_i}$ generates a new sample $f(S_i) \in R^{p \times W}$, where W is the dimensionality of the used *similarity* function (e.g., when comparing two multivariate time series, it may be useful to calculate the pairwise similarity between each variable rather than enforcing a single value to compare the whole sample). Finally, we redefine $L_r(S_i, S'_i)$ as:

$$L_r(S_i, S'_i) = \frac{1}{p} \sum_j (f(S_i)_j - f(S'_i)_j)^2$$

where $f(S_i)$ and $f(S'_i)$ are transformed representations of S_i and S'_i . Intuitively, this new error will be minimized if samples remain *relatively similar* to the pivot points in the reconstructed space, even if the space as a whole has changed.

To better illustrate our point, we will define our domain’s *similarity* with the Euclidean distance. While we do not employ it in the time series domain, we will use it in the following explanations due to its intuitive value. Thus, we formally define a *rigid transformation* as a transformation that satisfies $Euc(L(X), L(Y))^2 = Euc(X, Y)^2$, where $L : R^n \rightarrow R^n$. In this context, L simply represents a linear transformation of a vector space. Since our transformed space will be solely composed of Euclidean distances, it will then be invariant to any *rigid transformation* applied to our initial space.

As an example, we can prove that a *translation* is a *rigid transformation*. By defining $L(w) : w \rightarrow w + v$ (a translation given by a vector v):

$$\begin{aligned} Euc(L(X), L(Y))^2 &= Euc(X + v, Y + v)^2 \\ &= (X + v - Y - v) \cdot (X + v - Y - v) \\ &= (X - Y) \cdot (X - Y) \\ &= Euc(X, Y)^2 \end{aligned}$$

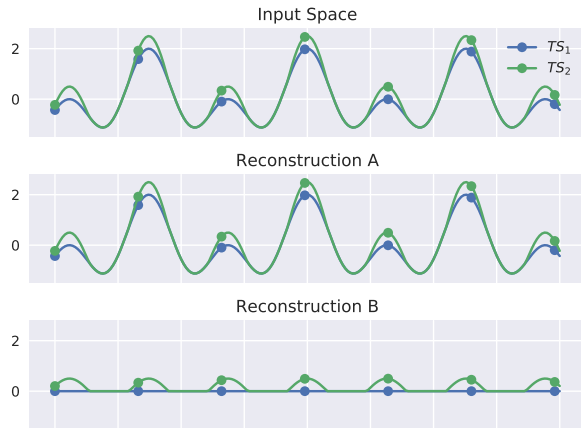


Figure 1: Alternative reconstructions of the input space. *Reconstruction A* would be the ideal reconstruction through a common AE, whereas *Reconstruction B* is a reconstruction allowed through our transformations. Both *Reconstruction A* and *Reconstruction B* have exactly the same L_r , with *Reconstruction B*’s representation being a rigid transformation of *Reconstruction A* ($h(w) : w \rightarrow w - v$, where $v = TS_1$).

By defining L accordingly, the same logic would immediately follow for rotations and, if the transformed space is normalized, we can also extend this property to uniform scaling. These transformations should not be confused with actually transforming the visual representations of our samples. A time series with n timestamps will be considered an n -dimensional vector and any transformation can be applied to any of its dimensions (timestamps) independently of the known temporal dependence. Fig. 1 illustrates this effect with a translation, and not only shows that our model can learn simplified representations of the input data, but also that its only constraint is to preserve *dissimilarities* between samples in the input space. The amount of *filtering* our model is allowed to perform will be mostly constrained by its complexity and latent space dimensionality. The simpler the model, the simpler the reconstructed space. This is true for any AE, but usually at the cost of an ever-increasing L_r , as the models stop being able to recreate all the nuances of the initial samples. Since we allow simpler representations to minimize L_r , we can achieve this with minimal penalty to the latent space quality (and potentially no penalty to L_r).

Leveraging Temporal Distance Metrics

Sound alternatives to the Euclidean distance for temporal data are DTW or SBD. While DTW is extremely well-known and popular for comparing time series, its complexity is quadratic on the dimensionality of the samples. There exist optimizations to the algorithm but, just like the original implementation, require parameter tuning for optimal results – a significant constraint in a completely unsupervised setting. On the contrary, SBD is specifically built for temporal data k-Shape (Paparrizos and Gravano 2015) and does not require any parameterization. It also generally provides bet-

Algorithm 1 Get clusters from embeddings obtained from projected space

```

1: procedure GENPROJSPACE( $S_{i=1}^N, P_{j=1}^P \subset S$ )
2:    $S' = \text{matrix}_{N \times p}$ 
3:   for each [sample, i] in  $S$  do
4:     for each [pivot, j] in  $P$  do
5:        $S'[i, j] = \text{Dist}(\text{sample}, \text{pivot})$ 
6:   return  $S'$ 
7: procedure GETCLUSTERS( $S_{i=1}^N, P_{j=1}^P \subset S, f_W, k$ 
   clusters)
8:    $S' = \text{GenProjSpace}(S, P)$ 
9:    $z = f_W(S')$ 
10:  clusters = kmeans( $z, k$ )
11:  return clusters

```

ter results than DTW and its variants, leading us to believe it is the best metric to report our results on. SBD is based on cross-correlation and uses coefficient normalization (i.e., between -1 and 1), independent of data normalization. The coefficient normalization divides the cross-correlation sequence by the geometric mean of autocorrelations of the individual sequences, as below:

$$SBD(\vec{x}, \vec{y}) = 1 - \max_w \left(\frac{CC_w(\vec{x}, \vec{y})}{\sqrt{R_0(\vec{x}, \vec{x})R_0(\vec{y}, \vec{y})}} \right)$$

where w is the position where the coefficient normalization is maximized, $CC_w(\cdot, \cdot)$ is the cross-correlation sequence with length $2m-1$ (i.e., $m = \text{length of } z_i$) and $R_0(\vec{x}, \vec{x}) = \sum_{l=1}^m x_l x_l$. SBD ranges from 0 to 2, with 0 representing perfect similarity between two sequences. Based on the definition of $CC_w(\cdot, \cdot)$, its temporal complexity is quadratic but, by using FFT, it can be reduced to $\mathcal{O}(m \log(m))$.

Due to the more complex nature of this measure, exploring the types of geometric transformations now allowed by our transformations would require a thorough analysis of their own, and will hence be left for future work. Regardless, it is equally easy to describe the invariance properties associated with the new generated transformations (explained in-depth in k-Shape): (1) scaling and translation; (2) shift; (3) uniform scaling; (3) occlusion; and (4) complexity. Although being invariant to different properties, the main premise of our transformation remains intact: a lower L_r will only be achieved by spaces in which samples remain *relatively similar* to the chosen pivot points (the only difference being in how *similarity* is calculated).

Tying It All Together

Drawing from our previously learned encoder mapping, f_W , the embeddings z_i of our AE are then fed into a classic clustering algorithm to group S into k clusters. This approach differs from other literature on unsupervised clustering by not relying on a KL divergence-based approach and instead generating latent spaces that preserve desirable domain-specific properties. We note the following: (1) using KL divergence requires defining a target probability distri-

bution that is specific to the domain, which has little generalization properties; and (2) any traditional clustering algorithm can still be used at this step (e.g., k-means) as the generated embeddings are already representative of the domain, clearly separating clusters as shown in Fig. 3. Even if our approach still requires us to pick a similarity metric, due to the nature of SBD this is a much smaller constraint because it requires no parameterization tuning. Nonetheless, other works have proposed methods for automatically deriving warping distances for a given input space (Abid and Zou 2018). This could allow us to further improve our transformations’ performance while remaining in a fully unsupervised setting but, given the complexity of this method alone, it will be left for future work.

In order to avoid generating transformations every time we calculate L_r during training, we apply these transformations directly on the input space, that is before even feeding them to the AE. Since $f(S)$ is already a simplified representation of our samples, it should allow for faster training and more robust results, but the optimization will only yield similar results if and only if $\frac{1}{N} \sum_i L_r(f(S_i), f(S'_i)) \Leftrightarrow \frac{1}{N} \sum_i L_r(f(S_i), f(S_i)')$. This means that the loss associated with transforming the reconstruction has to be equivalent to the loss of reconstructing the transformations. This should intuitively be true if our model is complex enough to accurately learn both S and $f(S)$ – driving our choice in the AE’s architecture (Fig. 2). The main inconvenience of this optimization is that we can no longer visualize the alternative representations learned by our AE, unless the assigned similarity metric is bijective (allowing full sample reconstruction from distances alone). Even if, for instance, we could achieve such a property by (i) defining Euclidean distance as our similarity metric and (ii) using $d + 1$ pivot points for d -dimensional samples, bijection is not a necessity. Truthfully, by using either DTW or SBD it might not even be a possibility (i.e., shown for DTW in (Tralie 2017)). Through our results, however, we show that not only can we ignore this property but also greatly reduce the number of required *pivot points* without sacrificing accuracy. The final clustering pipeline can be found in lines 7–11 in Alg. 1.

Finally, and to expand on the AE’s architecture, the first three levels consist of 2D convolution layers, which extract key short-term features, each followed by a max pooling layer of size P . The goal is to cast the time series into a more compact representation while retaining the relevant information. This dimensionality reduction is crucial for further processing to avoid very long sequences which can lead to poor performance. Leaky rectifying linear units (L-ReLU) are used. These activations are then fed to a gated recurrent unit (GRU) to obtain the latent representation. Using recurrent neural networks in the AE is inspired by their successful application to sentiment classification (Dai and Le 2015) and machine translation (Sutskever, Vinyals, and Le 2014), while the use of convolutional networks has been shown to be effective when dealing with temporal data in (Lin, Chen, and Yan 2013). This allows for the input to be collapsed in all dimensions except temporal. More specifically,

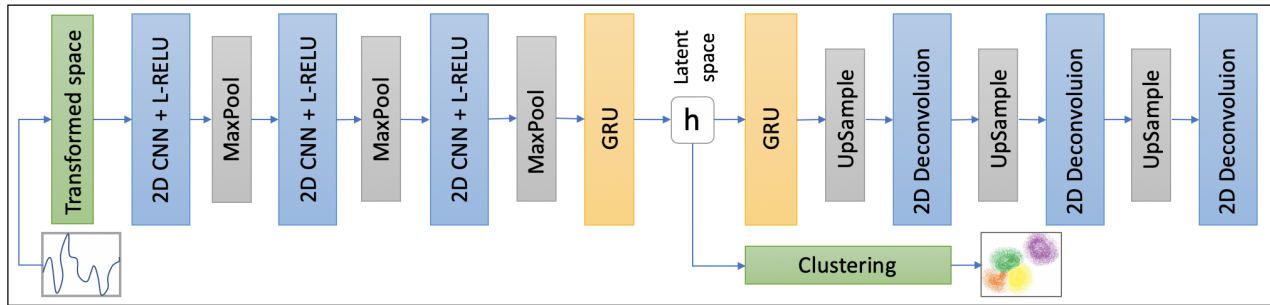


Figure 2: Schematic architecture of our approach. Spatially transformed inputs are processed through a multi-layer CNN-GRU symmetric AE. The encoder produces a latent representation h , which is then fed to a clustering layer.

the embeddings capture overarching features of the time series, while learning to ignore outliers and sampling rates, as shown in (Abid and Zou 2018). Reconstruction is provided by a GRU layer, followed by three upsampling layers of size P interleaved with three deconvolutional layers.

Evaluation

Setup

Parameter initialization – Because unsupervised clustering does not allow for determining the network’s optimal hyperparameters through cross-validation, we use typical default parameters and ignore any dataset-specific tuning. We set the filter sizes to 16, 32 and 64 for the first, second and third convolution layers, respectively. The kernel size is set to 4×4 across all layers, the pooling size is set to 5×5 and the latent space dimensions to 10. Finally, we use L-RELU activation functions for each layer with gradient $\alpha = 0.1$, the Adam optimizer with batch size = 256 and learning rate = 0.001, and train for 200 epochs. Our implementation is in Keras.

Accuracy measure – We use the labels in the datasets to compute the accuracy of the clustering, as in DEC. Essentially, the metric finds the best matching between a ground truth label and a cluster assignment. An optimal mapping can be done with the Hungarian algorithm (Kuhn 1955).

Datasets – We evaluate the performance of our approach on a collection of time series datasets from various domains, taken from the *UCR Time Series Classification Archive* (Chen et al. 2018). In addition, we also use the Australian Sign Language (ASL) dataset (Kadous 1999), which was used in (Chen, Ozsu, and Oria 2005) to test the EDR distance metric. Like the authors of Autowarp (Abid and Zou 2018), we use a subset consisting of $N = 50$ time series of length $T = 53$ from 10 different classes of signals. As opposed to the UCR datasets, which are univariate, ASL is multivariate, as measurements are provided as (x,y,z) coordinates along with the rotation of the palm.

Accuracy

We compare against two baselines that reflect the main observations previously discussed:

1. OS (Original Space) – classic clustering algorithms, such as k-means with Euclidean ($k\text{-means+EUC}$), k-means

with DTW ($k\text{-means+DTW}$), k-shape ($k\text{-shape}$), spectral ($spectral$) or DBSCAN ($dbscan$) are applied directly on the input time series data;

2. LS (Latent Space) – raw time series are collapsed into a 5-dimension latent representation via a dense denoising AE (Xie, Girshick, and Farhadi 2016) and then fed into $k\text{-means+EUC}$, $spectral$ or $dbscan$ (i.e., note that applying $k\text{-means+DTW}$ and $k\text{-shape}$ on the latent representation would bring no benefits, since the obtained embeddings are in Euclidean space).

An intuitive approach is to project the time series into an affine invariant space and then apply the same clustering algorithms as for LS on the transformed space. We denote it as P_r and also provide results for this approach. Finally, our methodology, P_r+LS , encompasses both affine invariant transformations and the use of a CNN-GRU AE, as described in Fig. 2. We use SBD in generating the projected space. The expectation is that by using projections with an AE that can extract temporal waveforms from the original time series, we will obtain superior performance relative to the baselines. Accuracy and standard deviation over 10 runs are shown in Table 1 for 7 UCR datasets and the ASL dataset. We also report improvements of P_r+LS and P_r over the OS and LS baselines (i.e., $acc_{P_r+LS|P_r} - \max(acc_{OS}, acc_{LS})$) relative to the $k\text{-means}$ and $spectral$ algorithms respectively. We make the following observations:

1. our approach consistently outperforms both baselines and P_r , either with $k\text{-means+EUC}$ or $spectral$ – this is best seen for dataset H (ASL), where accuracy reaches 82% for P_r+LS with $spectral$, while the baseline models are around low-40s to mid-60s;
2. improvements are more significant relative to OS and LS, and lower compared to P_r , which matches our initial intuition;
3. improvements over P_r are always positive, thus justifying the need of a multi-layer CNN-GRU AE in addition to generating transformations;
4. P_r+LS achieves the lowest standard deviation in the majority of cases (i.e., 1-3% for datasets A-F and H), which in turn shows a high degree of robustness;

	Model	A	B	C	D	E	F	G	H
OS	k-means+EUC	51.6±5	61.6±4	51.5±2	55.2±2	83.3±7	53±3	64.6±10	35.5±5
	k-means+DTW	55.8±6	64.1±5	50.5±2	55±2	83.8±7	63±3	55±11	41.4±6
	k-shape	52.6±6	58.2±3	54.7±14	52.7±1	64.7±7	51±1	49±4	41±8
	spectral	51.6±5	59±4	52.6±5	54.6±1	82.8±8	51.5±2	40±5	43±4
	dbscan	50±4	44.7±5	58.2±10	49.7±2	18±3	50±2	16.6±4	31±7
LS	k-means+EUC	52±4	55±4	64±4	55±1	83.3±2	52±1	57±5	60±4
	spectral	52.4±3	61±4	59.3±6	54.5±1	83.3±2	54±2	41±6	55±4
	dbscan	34±4	59.3±3	48±8	60.7±2	85.7±1	50±2	16.6±4	47±5
Pr	k-means+EUC	62.8±4	61.1±5	71.4±1	60.6±1	87±2	81.5±2	79±7	65±3
	spectral	56.4±3	59.3±4	54.5±2	64±1	92.3±3	83.5±1	67±8	63±4
	dbscan	35.2±3	65±4	53±3	64.5±2	77±2	50±1	17±5	55±3
	Impr. [OS/LS] [k-means]	7	-3	7.4	5.4	3.2	18.5	14.4	5
	Impr. [OS/LS] [spectral]	4	-1.7	-4.8	9.4	9	29.5	26	8
Pr+LS	k-means+EUC	67.6±2	70±2	78±1	66.7±1	94.4±1	85.5±1	84±5	78±2
	spectral	66.4±2	72.8±3	64±3	65.1±1	93.8±2	84.7±1	73±5	82±2
	dbscan	41.2±1	70.2±2	61±2	65.2±2	87±2	55±2	23±4	72±2
	Impr. [OS/LS] [k-means]	11.8	5.9	14	11.5	10.6	22.5	19.4	18
	Impr. [OS/LS] [spectral]	14	11.8	4.7	10.5	10.5	30.7	32	27

Table 1: Accuracy (mean and standard deviation over 10 runs) for our approach (Pr+LS) and Pr, compared to two baselines: OS and LS, when 16 pivot points are used to generate the projected space. For each dataset, we indicate k = number of clusters, n = number of samples and t = time series length, as follows: **A** = Computers(2,500,720), **B** = ECG5000(5,5000,140), **C** = ItalyPowerDemand(2,1096,24), **D** = PhalangesOutlinesCorrect(2,2658,80), **E** = Plane(7,210,144), **F** = ShapeletSim(2,200,500), **G** = SyntheticControl(6,600,60) and **H** = ASL(10,50,53).

5. mostly, Pr+LS with k-means+EUC outperforms all others models (up to 14% improvement over Pr+LS with spectral);
6. dbscan is significantly less stable than spectral and k-means+EUC and highly depends on the characteristics of the underlying dataset. For most datasets its improvement with Pr+LS is modest over the baselines or Pr (i.e., 5-7%), except for dataset A where it underperforms compared to OS by 9% and datasets E and H where it outperforms the baselines by 69% and 41%, respectively. For this reason, we do not include the improvement relative to dbscan in Table 1;
7. dbscan outperforms spectral and k-means+EUC for Pr for datasets B and D, which is to be expected given that this algorithm is particularly suited for outlier detection (i.e., applicable for both datasets). However, this advantage does not apply when projections are used in combination with our CNN-GRU AE;
8. with the baselines, k-shape is outperformed by either k-means or spectral, therefore we do not consider it in computing the improvements.

To shed light on what happens across these datasets, we briefly discuss some of their properties. On the one hand, dataset D (PhalangesOutlinesCorrect) is often used for anomaly detection of hand and bone outlines and has two clusters. Both clusters' distributions show identical anomalies towards the tail of the time series. This is why the baseline models perform only slightly better than random (i.e., accuracies between 50% and 55%). However, by projecting the original time series and generating an effective latent representation, we are able to boost performance to

66.7%, obtaining an improvement of 11.5% over the best performing k-means+EUC model. Similar behavior of the underlying distributions is observed for datasets C (ItalyPowerDemand) and F (ShapeletSim), without any presence of anomalies. In these cases, our approach achieves significant improvements of 14% and 22.5%, respectively. On the other hand, dataset E (Plane) shows different shapes of the time series belonging to different clusters, which explains why already with most of the baseline models we achieve over 80% accuracy. At the same time, Pr+LS with k-means+EUC and spectral reach 94% accuracy. In the case of dbscan, accuracy is only 18% when applied on the original time series, whereas using LS, Pr or Pr+LS boosts accuracy by even 69%. This is due to the fact that dbscan can only handle datasets with single density (Ding et al. 2015).

Finally, datasets A (Computers), B (ECG5000), G (SyntheticControl) and H (ASL) are exponents of similar underlying patterns – some of the clusters are easily distinguishable from one another, while others are extremely similar. For example, dataset G contains six different classes of control charts (e.g., increasing/decreasing trend, upward/downward shift). This dataset showcases an interesting property of our approach. Some clusters could be obtained from others via geometric operations on the feature space, like rotations, so one would expect our invariant models to perform worse. However, our models are invariant to these operations **on the whole space** (not on a sample-by-sample basis), and outperform the baselines in all cases.

In Fig. 3 we compare the latent representation generated by the LS model (i.e., recall that the AE used here is a denoising dense AE, as defined in DEC), with those obtained

with Pr+LS , when either DTW and SBD are used as metrics in computing the projections. In all three cases, we apply k-means+EUC as the final clustering step. An accuracy of 84% is achieved by using SBD (as reported in Table 1), whereas with LS performance is only at 57%. These results are explained by how well separated clusters are with SBD (Fig. 3b) compared to a simple AE (Fig. 3a), and even to using DTW instead (Fig. 3c), which performs 12% worse.

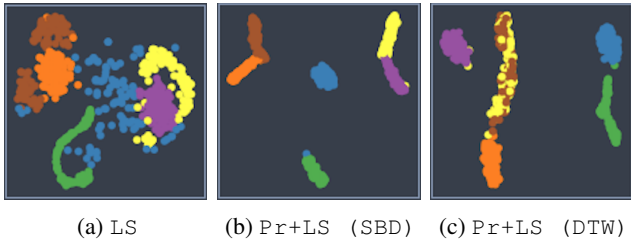


Figure 3: Latent representations after 200 epochs for the LS and Pr+LS models, when k-means+EUC is used as a final clustering step. For Pr+LS , we compare the resulting embeddings when DTW and SBD are used.

Sensitivity to number of pivot points

To generate the projected space for Pr+LS , we pick p random *pivot points* from the initial dataset and represent every sample as its similarity to each pivot point. We show accuracy and standard deviation results for $p \in \{4, 8, 16, 32\}$, when SBD is used, in Fig. 4. We omit results for DTW, since they show similar trends. In terms of accuracy, on the one hand, we note that for datasets A, B, C, D and F, differences in accuracy are marginal (2%, 5%, 2%, 1%, 4%), considering the standard deviation as well. On the other hand, for datasets E, G and H accuracy increases steadily with p , by 12.4%, 15.5% and 7% respectively. Across all datasets standard deviation decreases as p increases which - coupled with increased (or relatively constant) accuracy - shows that the preferred number of pivot points is 16 or 32. Naturally, p can take values greater than 32. We evaluated the evolution of accuracy and standard deviation in such cases but noticed that while standard deviation reduces *slightly*, the accuracy does not improve any further.

One possible improvement to randomly selecting pivot points would be to leverage optimal stopping theory (Bruss and others 2003). In that scenario we would introduce a slight overhead in picking optimal pivots but we would only need to have $p \approx k$ (as many pivots as the number of clusters), lowering overall temporal complexity while maintaining low standard deviation and high accuracy.

Computation cost

A secondary advantage of our approach, apart from the superior accuracy, is its low overhead through the optimization previously described (i.e., applying transformations directly on the input space as a pre-processing step). Given this, the overall added complexity is $\mathcal{O}(N \cdot p \cdot C)$, where N is the number of samples, p is the number of pivot points and C is

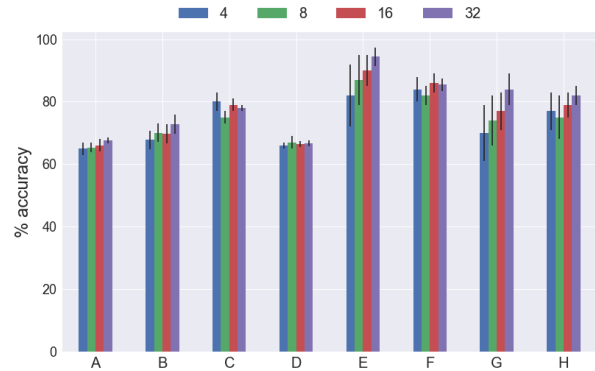


Figure 4: Accuracy and standard deviation for datasets A-H when $p = \{4, 8, 16, 32\}$ pivot points are used to generate the projected space.

the complexity of the selected similarity metric. We note the following: (i) p will be a constant with a value much lower than N , as previously shown in the sensitivity analysis, and (ii) C can be relatively low as the algorithm is not dependent on the selected similarity metric, as reflected in the accuracy results. These observations lead to a complexity growth that is linear on the number of samples, namely $\mathcal{O}(N \cdot C)$.

We measure the time required to generate the transformations with either DTW or SBD as the similarity metric, when $p = 16$ pivot points are used. For instance, for dataset C, both times are comparable (1s), while for datasets D, E, F and G, using DTW incurs execution times 3 to 32 times higher than in the case of SBD (i.e., (32s, 5s, 67s, 3s) compared to (1s, 1s, 5s, 1s)). All experiments were run on CPUs only, without any dedicated hardware (either GPU or onboard graphics). Each of the CPUs has 12 virtual cores clocked at $\sim 2.33\text{GHz}$.

Conclusions

In this paper, we tackle the problem of clustering temporal data. While a plethora of traditional, time series specific and more recent deep learning-based clustering methods exist, they suffer from important drawbacks when both varying sampling rates and high dimensionality (i.e., long sequences) are present in the input data.

Therefore, we propose a novel approach in which we first transform the time series into a distance-based projected representation by using elastic metrics (DTW) or cross-correlation measures (SBD) suitable for dealing with temporal data. Then, we feed these projections into a multi-layer CNN-GRU AE in order to generate meaningful latent representations, that allow for a natural separation of clusters with any Euclidean distance-based clustering algorithm. Evaluation on multiple univariate and multivariate time series datasets from various domains shows that our approach is robust and outperforms existing methods in all cases: up to 32% for spectral clustering, and up to 22.5% for k-means clustering. The computational overhead of our method is negligible.

References

- [Abid and Zou 2018] Abid, A., and Zou, J. 2018. Autowarp: Learning a warping distance from unlabeled time series using sequence autoencoders. *NeurIPS*.
- [Aggarwal and Reddy 2014] Aggarwal, C. C., and Reddy, C. K. 2014. *Data Clustering: Algorithms and Applications*. CRC Press.
- [Aghabozorgi, Shirkhorshidi, and Wah 2015] Aghabozorgi, S.; Shirkhorshidi, A.; and Wah, T. Y. 2015. Time-series clustering - a decade review. 16–38.
- [Aljalbout et al. 2018] Aljalbout, E.; Golkov, V.; Siddiqui, Y.; Strobel, M.; and Cremers, D. 2018. Clustering with deep learning: Taxonomy and new methods. *arXiv preprint arXiv:1801.07648v2*.
- [Besse et al. 2015] Besse, P.; Guillouet, B.; Loubes, J.-M.; ; and François, R. 2015. Review and perspective for distance based trajectory clustering. *arXiv preprint arXiv:1508.04904*.
- [Bruss and others 2003] Bruss, F. T., et al. 2003. A note on bounds for the odds theorem of optimal stopping. *The Annals of Probability* 31(4):1859–1961.
- [Chazan, Gannot, and Goldberger 2018] Chazan, S. E.; Gannot, S.; and Goldberger, J. 2018. Deep clustering based on a mixture of autoencoders. *arXiv preprint arXiv:1812.06535v1*.
- [Chen and Ng 2004] Chen, L., and Ng, R. 2004. On the marriage of lp-norms and edit distance. *Proceedings of the Thirtieth International Conference on Very Large Databases* 792–803.
- [Chen et al. 2018] Chen, Y.; Keogh, E.; Hu, B.; Begum, N.; Bagnall, A.; Mueen, A.; and Batista, G. 2018. The ucr time series classification archive.
- [Chen, Ozsü, and Oria 2005] Chen, L.; Ozsü, T.; and Oria, V. 2005. Robust and fast similarity search for moving object trajectories. *Proceedings of the 2005 ACM SIGMOD International Conference on Management of Data* 491–502.
- [Dai and Le 2015] Dai, A. M., and Le, Q. V. 2015. Semi-supervised sequence learning. *NeurIPS* 3079–3087.
- [Ding et al. 2015] Ding, R.; Wang, Q.; Dang, Y.; Fu, Q.; Zhang, H.; and Zhang, D. 2015. Yading: Fast clustering of large-scale time series data. *Proceedings of VLDB* 8(5).
- [Dizaji et al. 2017] Dizaji, K. G.; Herandi, A.; Deng, C.; Cai, W.; and Huang, H. 2017. Deep clustering via joint convolutional autonecoder embedding and relative entropy minimization.
- [Guo et al. 2017] Guo, X.; Gao, L.; Liu, X.; and Yin, J. 2017. Improved deep embedded clustering with local structure preservation. *IJCAI*.
- [Kadous 1999] Kadous, M. W. 1999. Australian sign language dataset. <http://kdd.ics.uci.edu/databases/auslan/auslan.data.html>.
- [Kuhn 1955] Kuhn, H. W. 1955. The hungarian method for the assignment problem. *Naval research logistics quarterly* 2:83–97.
- [Langkvist, Karlsson, and Loutfi 2014] Langkvist, M.; Karlsson, L.; and Loutfi, A. 2014. A review of unsupervised feature learning and deep learning for time-series modeling. *Pattern Recognition Letters* 42:11–24.
- [Lin, Chen, and Yan 2013] Lin, M.; Chen, Q.; and Yan, S. 2013. Network in network. *arXiv preprint arXiv:1312.4400*.
- [Malhotra et al. 2017] Malhotra, P.; TV, V.; Vig, L.; Agarwal, P.; and Shroff, G. 2017. Timenet: Pre-trained deep recurrent neural network for time series classification. *arXiv preprint arXiv:1706.08838*.
- [Paparrizos and Gravano 2015] Paparrizos, J., and Gravano, L. 2015. k-shape: Efficient and accurate clustering of time series. *SIGMOD* 69–76.
- [Sakoe and Chiba 1978] Sakoe, H., and Chiba, S. 1978. Dynamic programming algorithm optimization for spoken word recognition. *IEEE Transactions on Acoustics, Speech, and Signal Processing* 26:43–49.
- [Shah and Koltun 2017] Shah, S. A., and Koltun, V. 2017. Deep continuous clustering. *arXiv preprint arXiv:1803.01449v1*.
- [Sutskever, Vinyals, and Le 2014] Sutskever, I.; Vinyals, O.; and Le, Q. V. 2014. Sequence to sequence learning with neural networks. *NeurIPS* 3104–3112.
- [Tralie 2017] Tralie, C. J. 2017. Self-similarity based time warping. *arXiv:1711.07513*.
- [Wang et al. 2013] Wang, H.; Su, H.; Zheng, K.; Sadiq, S.; and Zhou, X. 2013. An effectiveness study on trajectory similarity measures. *Proceedings of the Twenty-Fourth Australasian Database Conference* 13–22.
- [Xie, Girshick, and Farhadi 2016] Xie, J.; Girshick, R.; and Farhadi, A. 2016. Unsupervised deep embedding for clustering analysis. *ICML* 198–202.
- [Yang et al. 2017] Yang, B.; Fu, X.; Sidiropoulos, N. D.; and Hong, M. 2017. Towards k-means-friendly spaces: Simultaneous deep learning and clustering. *arXiv preprint arXiv:1610.04794v2*.
- [Yang, Parikh, and Batra 2016] Yang, J.; Parikh, D.; and Batra, D. 2016. Joint unsupervised learning of deep representations and image clusters. *arXiv preprint arXiv:1604.03628v3*.
- [Yin et al. 2014] Yin, H.; Qi, H.; Xu, J.; Hung, W. N.; and Song, X. 2014. Generalized framework for similarity measure of time series. *Mathematical Problems in Engineering*.
- [Zhang et al. 2017] Zhang, D.; Sun, Y.; Eriksson, B.; and Balzano, L. 2017. Deep unsupervised clustering using mixture of autoencoders. *arXiv preprint arXiv:1712.07788v2*.